Axial resolution of laser optoacoustic imaging: Influence of acoustic attenuation and diffraction

Rinat O. Esenaliev [1], Herve Alma [2], Frank K. Tittel [2], and Alexander A. Oraevsky [3*]

[1] Biomedical Engineering Center, Department of Physiology and Biophysics, The University of Texas Medical Branch, Galveston, TX 77555

[2] Department of Electrical and Computer Engineering, Rice University, Houston TX 77005

[3] Biomedical Engineering Center, Department of Ophthalmology and Visual Sciences, The University of Texas Medical Branch, Galveston, TX 77555
phone: (409)-772-8348, FAX: (409)-772-0751, e-mail: <alexander.oraevsky@utmb.edu>

ABSTRACT

Laser optoacoustic imaging can be applied for characterization of layered and heterogeneous tissue structures *in vivo*. Accurate tissue characterization may provide: (1) means for medical diagnoses, and (2) pretreatment tissue properties important for therapeutic laser procedures. Axial resolution of the optoacoustic imaging is higher than that of optical imaging. However, the resolution may degrade due to either attenuation of high-frequency ultrasonic waves in tissue, or/and diffraction of low-frequency acoustic waves. The goal of this study was to determine the axial resolution as a function of acoustic attenuation and diffraction upon propagation of laser-induced pressure waves in water with absorbing layer, in breast phantoms, and in biological tissues. Acoustic pressure measurements were performed in absolute values using piezoelectric transducers. A layer or a small sphere of absorbing medium was placed within a medium with lower optical absorption. The distance between the acoustic transducer and the absorbing object was varied, so that the effects of acoustic attenuation and diffraction could be observed. The location of layers or spheres was measured from recorded optoacoustic pressure profiles and compared with real values measured with a micrometer. The experimental results were analyzed using theoretical models for spherical and planar acoustic waves. Our studies demonstrated that despite strong acoustic attenuation of high-frequency ultrasonic waves, the axial resolution of laser optoacoustic imaging may be as high as 20 μm for tissue layers located at a 5-mm depth. An axial resolution of 10 μm to 20 μm was demonstrated for an absorbing layer at a distance of 5 cm in water, when the resolution is affected only by diffraction. Acoustic transducers employed in optoacoustic imaging can have either high sensitivity or fast temporal response. Therefore, a high resolution may not be achieved with sensitive transducers utilized in breast imaging. For the laser optoacoustic imaging in breast phantoms, the axial resolution was better than 0.5 mm.

Key words: thermal stress, laser ultrasound, acoustic transducer, cancer detection, tissue characterization.

1. INTRODUCTION

Applications of optical imaging for detection and localization of diseased tissues have been intensively investigated for the last decade (see, for instance, SPIE and OSA Proceedings[1,2]). Optical imaging is based on differences in optical properties between normal and abnormal tissues. The contrast in optical properties is greater than contrast in acoustic properties. However, the sensitivity and the resolution of optical imaging are limited by the light scattering in tissues.

Ultrasound imaging is a widely used clinical technique for tissue characterization[3]. It is based on reflection of ultrasonic waves from acoustic inhomogeneities in tissues. Ultrasonic waves can propagate in tissues significantly deeper with minimal attenuation and distortion compared with optical waves[4]. Resolution of ultrasound imaging is often acceptable, especially when performed at higher frequencies. The major limitation of the ultrasonic imaging is its low contrast in soft tissues.

SPIE Vol. 3254 • 0277-786X/98/$10.00

Laser optoacoustic imaging combines advantages of optical and ultrasound imaging in one technology[5]. It is based on optical contrast and time-resolved detection of laser-induced ultrasonic waves. The laser-induced ultrasonic waves in tissues are generated by the thermoelastic mechanism and resembles profile of thermal energy distribution in the irradiated volume (see, for example, [6,7]). Laser optoacoustic imaging system can operate in two modes, suitable for deep (up to 7 cm) and subsurface (up to 4 mm) imaging[5,8]. Application of sensitive acoustic transducers allows detection of millimeter-sized optical inhomogeneities in strongly scattering media simulating biological tissues[9]. Recently, detection of a small (2 mm) phantom tumors was demonstrated with the use of the laser optoacoustic imaging system (LOIS) at the depth of 60-mm within a breast phantom (μ_{eff} = 1.0 cm^{-1})[10].

Resolution limits for the laser optoacoustic imaging has been studied, but not thoroughly[11,12]. In general, theoretical limit of z-axial (in depth) resolution is defined by the temporal response of acoustic transducers and the detection system, and by the laser pulse duration. However, resolution of LOIS may also be limited due to distortion of ultrasonic pulses by the following processes (1) diffraction of acoustic waves that occurred upon propagation in tissues and in acoustic detectors, and (2) attenuation of acoustic waves in tissues. Diffraction and attenuation may widen the ultrasonic pulses and shift their positions in measured pressure profiles. Therefore, location and dimensions of the objects or layers in optoacoustic images will be measured inaccurately. The goal of this study was to understand the influence of acoustic diffraction and attenuation on z-axial resolution of laser-optoacoustic imaging, i.e. on accuracy of localization and dimension measurements.

2. THEORETICAL BACKGROUND

2.1. Generation and detection of laser-induced acoustic waves.

Two different cases of laser optoacoustic imaging were considered in this study: (1) optoacoustic imaging utilizing detection of spherical waves and (2) optoacoustic imaging utilizing detection of plane waves. Spherical acoustic waves can be emitted by small acoustic sources such as deeply located tumors in the breast, brain, and other organs. In this case, laser irradiation and acoustic wave detection are usually performed from opposite sides of the investigated organ. This type of imaging is called imaging in forward mode because detected acoustic waves propagate along the direction of incident laser radiation (Fig. 1a, b). The optoacoustic imaging in forward mode was used in this study to detect model tumors in breast phantom.

Plane acoustic waves can be emitted by subsurface tissue layers in the skin, arteries, or hollow organs. Both the laser irradiation and acoustic wave detection can be performed *in vivo* at one and the same side of the investigated organ. This type of imaging is called optoacoustic imaging in backward mode because detected acoustic waves propagate in the direction opposite to the direction of incident laser radiation (Fig. 1c).

Detection of plane acoustic waves in the forward mode can be used in the cases of (1) thin tissues *in vivo*, (2) tissues *in vitro* which can be prepared as thin slices, and (3) in model experiments. In this study plane waves from tissues *in vitro* and from a phantom tissue layer (optical filter) were detected in the forward mode.

Maximal contrast, resolution and sensitivity of laser optoacoustic imaging can be obtained, if the irradiation conditions of temporal stress confinement are satisfied[6]. In this case, maximal efficiency of thermoelastic pressure waves is achieved and distribution of laser-induced acoustic sources resembles distribution of absorbed energy deposition. Laser radiation with nanosecond pulses is usually applied to satisfy the irradiation conditions of temporal stress confinement in the irradiated volume.

Generated pressure wave. A pressure rise distribution P(**r**) upon stress-confined irradiation condition is expressed as:

$$P_{gen}(\mathbf{r}) = \Gamma(\mathbf{r})\mu_a(\mathbf{r})F(\mathbf{r}) \qquad (1)$$

where $\Gamma(\mathbf{r})$ is the Grüneisen coefficient which is dependent on mechanical and thermophysical parameters of tissue, $\mu_a(\mathbf{r})$ is the absorption coefficient, and F(**r**) is the fluence distribution in the tissue. This general formula is valid for any type of laser optoacoustic imaging.

Detected pressure wave. An amplitude of detected pressure wave is dependent on tissue type and detection geometry. In case of an absorbing sphere deeply located within the irradiated tissue, it can be calculated by the formula[13]:

$$P_{\text{det, sph}} = \frac{P_{gen}}{2}\frac{r_o}{R} \qquad (2)$$

where r_0 is the sphere radius, R is the distance between the sphere and acoustic detector. The ratio r_0/R is due to spherical propagation of acoustic waves from the source. The pressure pulse from the spherical source will have a bipolar N-shaped profile[14, 15].

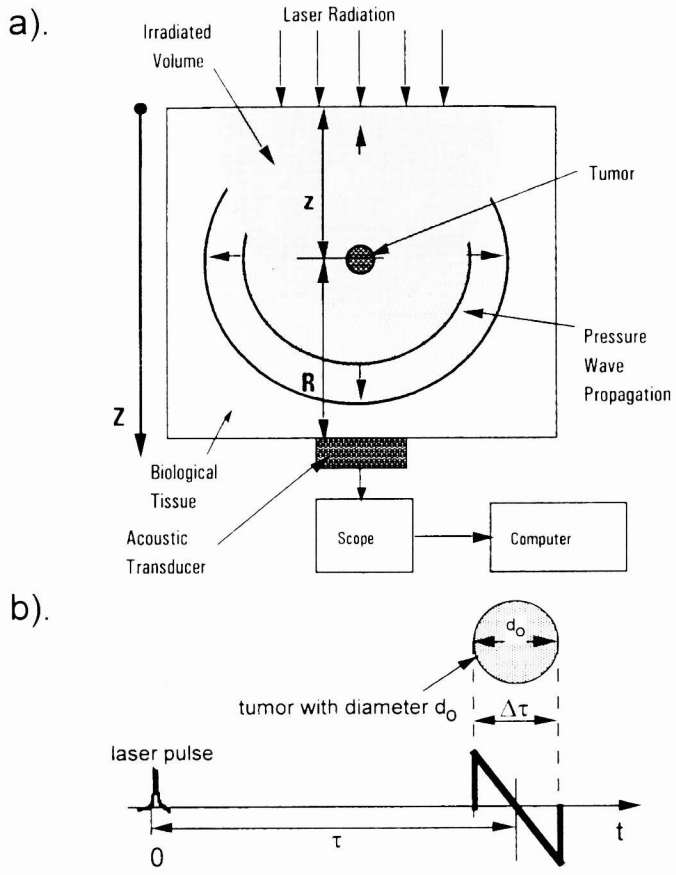

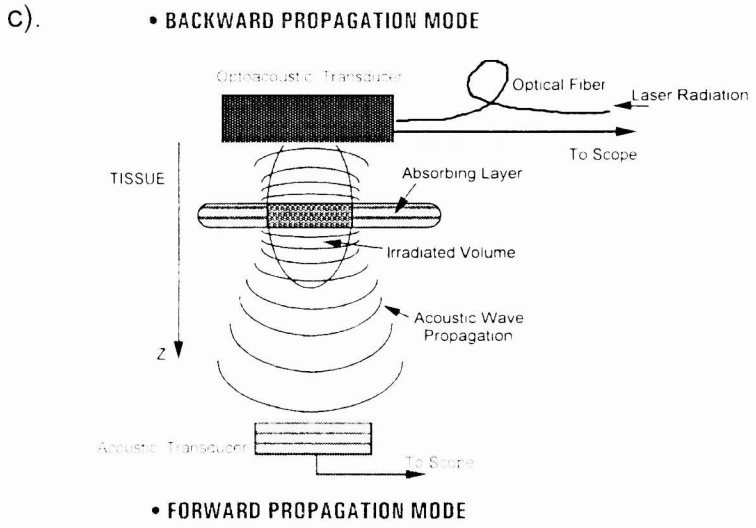

Figure 1. Schematics of optoacoustic imaging utilizing spherical wave detection in forward mode (a); Pressure profile from a spherical source (b); Schematics of optoacoustic imaging utilizing plane wave detection in forward and backward modes (c).

In the case of an acoustic source emitting plane waves, the detected pressure amplitude is expressed by the formula:

$$P_{\mathrm{det},pl} = P_{gen} / 2 \tag{3}$$

where factor 1/2 is due to propagation of two plane waves in two opposite directions from the source. Formulae (2) and (3) are valid if acoustic diffraction and attenuation are negligible.

Distance between acoustic source and transducer. It is necessary to measure the distance between an acoustic source and a transducer to localize the source and reconstruct its image. For any type of optoacoustic imaging this distance is given by the formula:

$$R = c_s \tau \tag{4}$$

where c_S is the speed of sound and τ is the temporal delay between the laser pulse and the signal from the source.

Dimensions of acoustic source. The dimensions of acoustic sources can be calculated by the formula:

$$d_0 = c_s \Delta\tau \tag{5}$$

where d_0 is either the sphere diameter in case of a spherical source, or the layer thickness in case of a layered source, and $\Delta\tau$ is the duration of acoustic pulses emitted by the source.

2.2. Distortion of acoustic waves.

Profile of laser-induced pressure waves can be distorted due to their diffraction and attenuation in tissue[6, 15, 16]. This may decrease the accuracy of dimension measurements and measurements of the distance between the source and detector. Therefore, the resolution of laser optoacoustic imaging may be influenced by these processes.

Influence of acoustic wave diffraction. Acoustic wave diffraction can substantially change profile of detected pressure[15, 16]. The pressure profile at the depth, z, distorted due to diffraction and detected perpendicular to the axis of propagation of the acoustic wave, $P(z, \tau, r_{\perp} = 0)$ and generated pressure profile, $P_{gen}(t)$, are related by the following expression[15]:

$$P_{diffr}(z,t,r_{\perp}=0) = P_{gen}(t) - \int_{-\infty}^{t} w_D exp(-w_D(t-t)) P_{gen}(t)dt \qquad (6)$$

where $\omega_D = 2c_S z/a_L^2$ is the diffraction frequency, and a_L is the laser beam diameter. Using (6), the generated pressure profile can be calculated by the formula:

$$P_{gen}(t) = P_{diffr}(t) + \int_{-\infty}^{t} w_D P_{diffr}(\tau)d\tau \qquad (7)$$

Therefore, the generated pressure profile can be reconstructed from the measured profile taking into account the diffraction effect.

Influence of acoustic wave attenuation. It is well known that acoustic attenuation coefficient, $\alpha(f)$, increases with the increase of frequency. The following relation is valid for tissues in a wide range of acoustic frequencies[17]:

$$\alpha(f) = af^b \qquad (8)$$

where a and b are factors that depend on tissue composition and structure. Typical value of b ranges between 1 and 2 for soft tissues.

Laser-induced acoustic waves have a wide frequency spectrum. Their spectral maximum is defined by the dimension of optoacoustic source, d_0, and estimated as:

$$f_{max} \sim c_S / d_0 \qquad (9)$$

Therefore, high-frequency acoustic waves (10 to 100 MHz) are generated in soft tissues, if the dimension of the acoustic source is of the order of 10 to 100 μm. The acoustic attenuation coefficient for these high-frequency waves may vary significantly (0.1 to 100 cm^{-1}) depending on tissue type[17].

The acoustic source with this dimensions can be either an absorbing volume (or layer) surrounded by other tissues with low absorption or a strongly absorbing tissue with high optical attenuation coefficient, μ_{eff}, of the order of 100 - 1000 cm^{-1}. Such high optical attenuation results in generation of pressure only in a thin subsurface layer with the thickness of the order of 10 - 100 μm.

High-frequency component of the generated pressure pulse will be attenuated stronger than the low-frequency component as depicted by expression (8). The acoustic attenuation can widen sharp edges of the pressure pulse with high-frequency spectrum. Therefore, attenuated pulse will be wider than the initially generated one. Furthermore, the amplitude of the high-frequency pressure pulse will decrease significantly. If pressure pulse propagates longer distances, the distortion of the pulse will be stronger.

Resolution of optoacoustic imaging will be decreased due to the pressure pulse broadening, because accuracy of localization and dimension measurement will be lower. The longer the propagation distance the lower the resolution.

Influence of acoustic detector dimension. The dimension of acoustic detectors may influence the profile of detected ultrasonic pulses and decrease resolution of optoacoustic imaging. For instance, if the distance between a spherical acoustic source and detector is comparable to the detector aperture, the detected pressure profile will be different from the pressure profile detected at a distance much greater than detector aperture.

3. MATERIALS AND METHODS

3.1. Laser sources.

Experiments on breast phantoms were performed with a Q-switched Nd:YAG laser with the following parameters: wavelength - 1064 nm, pulse duration - 10 ns, pulse energy - 50 mJ, diameter of laser spot - 8 mm, fluence - 100 mJ/cm^2. Third harmonic of a Q-switched Nd:YAG laser was used for experiments on acoustic diffraction. The parameters of laser radiation were: wavelength -532 nm, pulse duration - 12 ns, pulse energy - 5 mJ, diameter of laser spot - 8 mm, laser fluence - 10 mJ/cm^2.

Experiments on acoustic attenuation were performed with an ArF-laser with the following parameters: wavelength - 193 nm, pulse duration - 11 ns, pulse energy - 100 mJ, laser beam diameter - 6.2 mm. Incident pulse energy was attenuated and equal to 0.118 mJ providing incident fluence of 0.39 mJ/cm^2.

Irradiation with these parameters can not induce any thermal or mechanical damage to the samples, because maximal temperature and pressure rise were less than 0.5° K and 5 bar, respectively.

3.2. Sample preparation and measurement procedures.

Breast phantoms were made of 10%-gelatin and had dimensions of 100 x 97 x 57 mm. The breast phantom that resemble optical properties of human breast and the phantom preparation procedure were previously described[10,16]. Attenuation coefficient in the phantoms was 1.0 cm^{-1} which is equal to the attenuation coefficient of the human breast *in vivo* in the in the near-infrared spectral range[20-21]. Polystyrene spheres or milk were used as scatterers. Bovine hemoglobin was used as an absorber to make spheres with enhanced absorption. Diameter of the spheres was varied from 2 to 6 mm. The sphere diameters and distance between them and acoustic transducer were calculated by the formulas (4) and (5), respectively, and compared with actual ones measured with a caliper. Irradiation scheme of the phantoms is presented in Figure 1a.

(a)

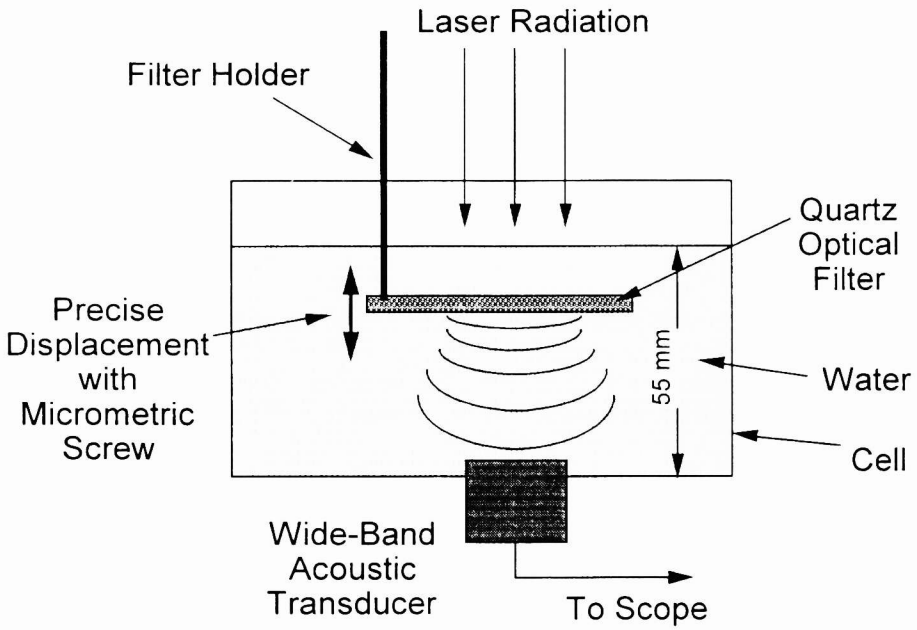

(b)

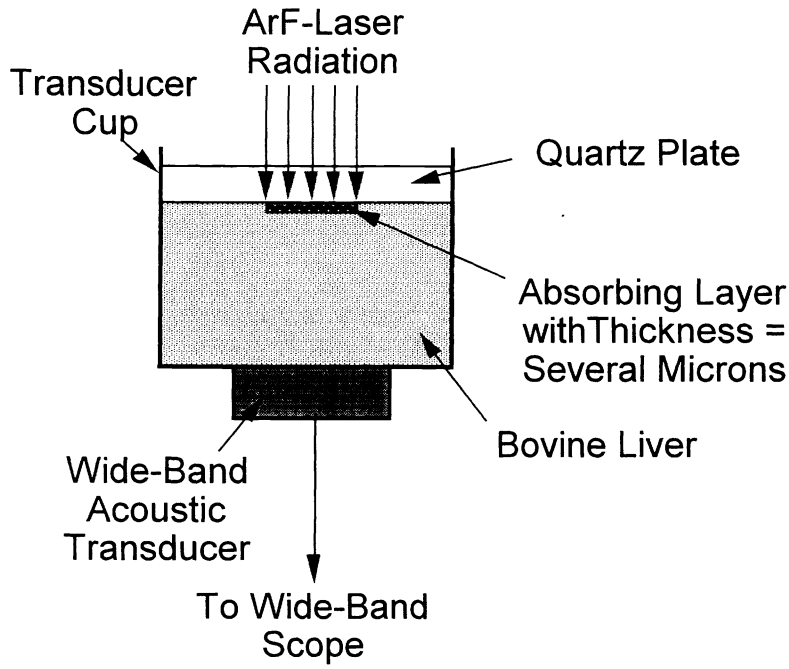

Figure 2. Experimental set up to study: (a) diffraction of optoacoustic waves, (b) attenuation of high-frequency optoacoustic waves in tissues.

A neutral density optical filter (thickness = 2 mm, μ_a = 32 cm^{-1} at λ = 532 nm) was used as a source of optoacoustic plane waves in the experiment on acoustic diffraction (Fig. 2a). The filter was embedded in water. The distance between the water surface and the transducer was 55 mm. Displacement of the filter was performed by a micrometric screw with the displacement accuracy of 1 μm. This allowed monitoring the distance between the irradiated filter surface and the transducer with the accuracy of 1 μm. Flat and smooth surface of the filter provided generation of optoacoustic wave with a planar front.

Optoacoustic signals were recorded at various distances between the filter and the transducer. This distance was calculated from the measured optoacoustic pressure profiles using formula (4) and compared with the distance determined with the micrometric screw.

Bovine liver slabs 50 x 50 mm with thickness from 0.060 to 5.0 mm were used in the acoustic attenuation experiment (Fig. 2b). The slabs were placed between a quartz plate and an acoustic transducer. The quartz plate surfaces were aligned parallel to the transducer surface and perpendicular to the incident laser beam. Optical quality of the quartz plate surface and fine alignment allow generation of a plane acoustic wave in the liver samples.

Typical attenuation coefficient in tissues is about several thousand cm^{-1} at the ArF-laser wavelength yielding penetration depth of several microns. Therefore, a thin subsurface layer with the thickness of several microns was an acoustic source in this case. Acoustic propagation time in this source was equal to several nanosecond which is less than laser pulse duration. That means that the conditions of temporal stress confinement are not satisfied. In this case the duration of the generated ultrasonic pulses is equal to the laser pulse duration[6] yielding acoustic wave frequency of the order of 100 MHz.

3.3. Acoustic transducers and detection systems.

High sensitivity of acoustic wave detection was required for the experiment on the breast phantoms. The profiles of laser-induced acoustic waves may be measured employing either piezoelectric transducers[18] or optical detection[19]. Our study utilized the piezoelectric detection. A specially designed sensitive acoustic transducer LBAT-14 (sensitivity - 2.5 V/bar, bandwidth - 2.5 MHz) with pre-amplifier was used in this experiment.

Broad-band acoustic transducers and detection system were needed for the acoustic diffraction and attenuation experiments. An acoustic transducer WAT-12 (Science Brothers Inc., Houston, TX) with sensitivity of 12 mV/bar and bandwidth of >100 MHz was used for the experiment on acoustic diffraction. High-frequency acoustic transducer WAT-04 (sensitivity - 10 mV/bar, bandwidth - 300 MHz) was applied for the experiment on acoustic attenuation. Signals from the transducer were recorded by a Tektronix scope (500 MHz bandwidth) and processed with a personal computer.

4. RESULTS

4.1. Breast phantom experiment.

Several different breast phantoms were used for this experiment. One of the pressure profiles obtained upon irradiation of the breast phantom with 2-mm and 4-mm spheres is presented in Figure 3. The first peak is caused by absorption of laser radiation in the acoustic transducer. It is used as a reference signal. The second signal is the signal from the 4-mm sphere. It has two maxima and one minimum. The next signal is signal from the 2-mm sphere. It has bipolar N-shaped profile typical for spherical sources.

The upper x-axis represents depth, z, from irradiated surface. The sharp edge at z=0 is caused by reflection of the laser-induced acoustic waves from gelatin-air interface. It indicates position of the surface. Wavelet filtering was used to increase of signal-to-noise ratio. The wavelet-filtered signal is also presented in the plot. Exponential slope representing background optoacoustic pressure was automatically subtracted from raw experimental signals by this filtering procedure.

Both diameter of the spheres and distance between the spheres and transducer were calculated from the measured profiles using formula (4) and (5). The calculated values were compared with the actual ones measured with a caliper. Table 1 represents the calculated and actual values of the distance between the spheres and transducer. The calculated and actual values of the sphere diameter are shown in the Table 2.

4.2. Acoustic diffraction experiment.

Pressure profiles recorded from the filter positioned at various distances from the transducer are presented in Figure 4. If the filter was at the distance of 5 mm to the transducer, the detected pressure profile is bipolar. It indicates that the diffraction is negligible and the pressure wave is planar. The second maximum appears with the increase of the distance between the filter and transducer. The diffraction is significant at the distance of 30 - 50 mm. The pressure profiles are plotted so that their first maxima coincide. In this case, the pressure pulse distortion due to diffraction is clearly seen.

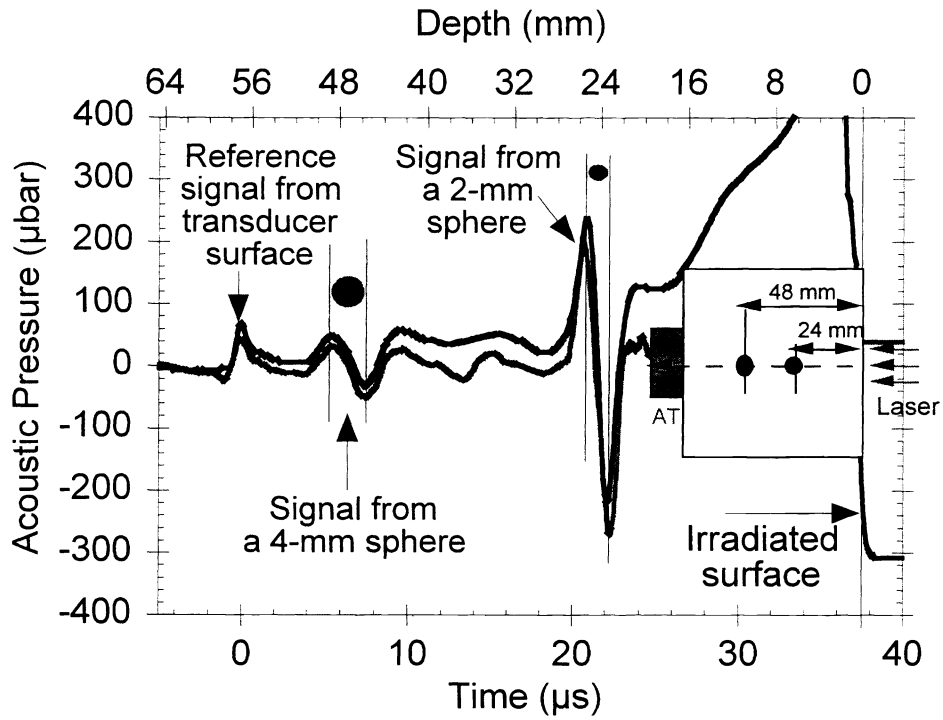

Figure 3. Optoacoustic signals from small spheres in the breast phantom (upper curve) and the same signal after wavelet processing (lower curve).

Table 1. Accuracy of localization of small spheres in the phantom.

Sphere Diameter (mm)	Measured Distance (mm)	Actual Distance (mm)	Δ (mm)	Δ/R (%)
2.0	39.2	39.0	0.2	0.5
4.0	74.3	74.0	0.3	0.4
6.0	76.5	76.0	0.5	0.7

Table 2. Accuracy of dimension measurement for small spheres in the phantom.

Sphere Diameter (mm)	Measured Diameter (mm)	Δ (mm)	Δ/d_0 (%)
2.0	2.16	0.16	8.0
4.0	3.5	0.5	12.0
6.0	5.5	0.5	8.3

Figure 5 depicts the acoustic arrival time, τ, as a function of distance between the irradiated surface of the filter and the transducer. The right y-axis represents this distance calculated from optoacoustic pressure profiles using the formula (4). There is a good agreement between the calculated and the actual distance. The location of the absorbing layer was determined with an accuracy of about 10 μm at the distances of 30 to 50 mm.

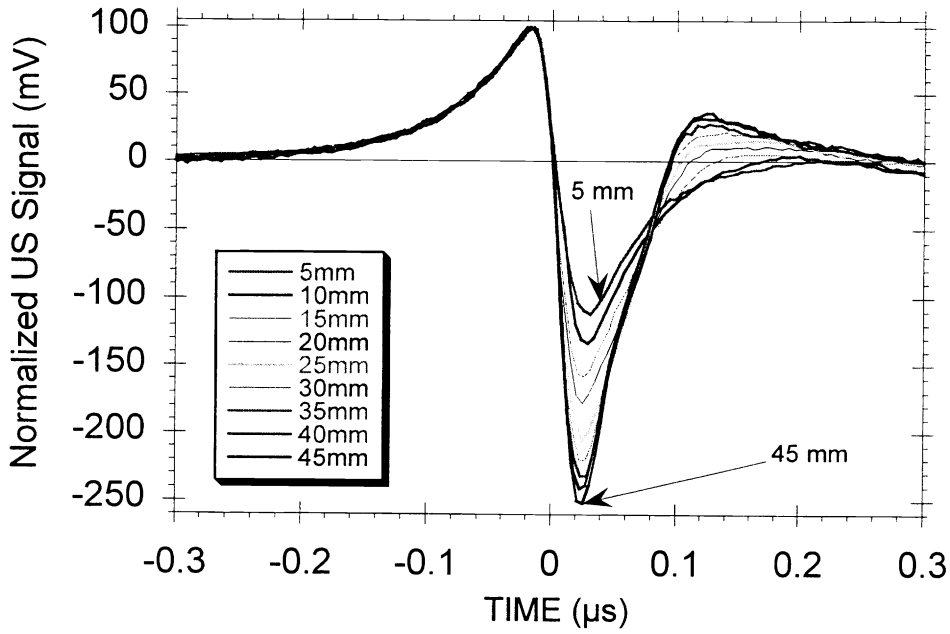

Figure 4. Optoacoustic signals at various distances between the filter and transducer.

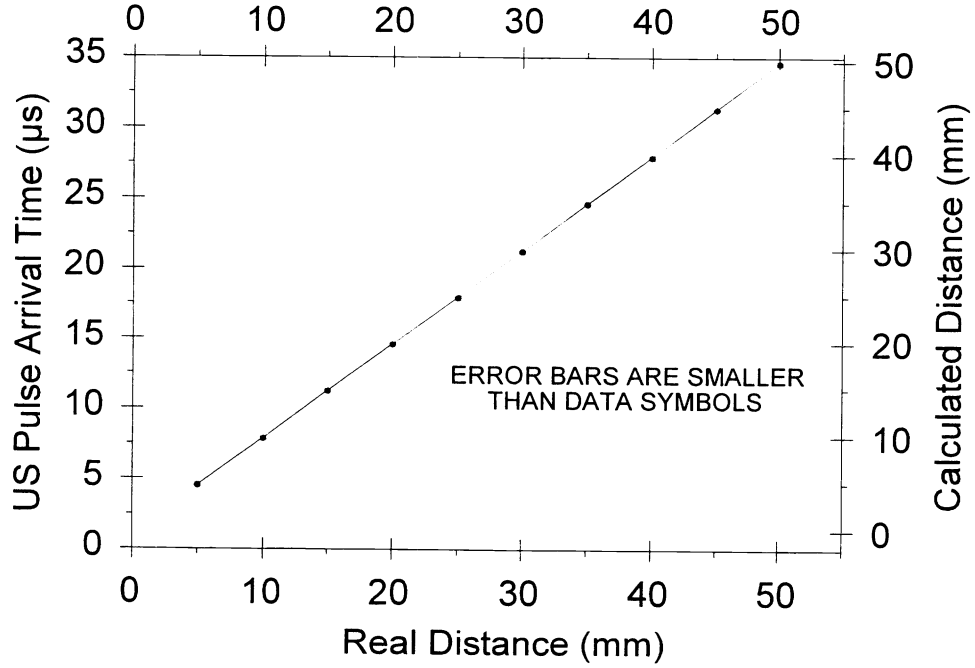

Figure 5. Acoustic arrival time and calculated distance vs. distance between the filter and transducer.

4.3. Acoustic attenuation experiment.

Pressure profiles from the liver samples with the thickness of 0.06 and 3.9 mm are presented in Figure 6. The pressure profile from the 0.06-mm liver sample has a duration of 11 ns which equals the laser pulse duration. The pressure profile amplitude from the 3.9-mm sample is substantually less than that measured from the thin sample. Furthermore, its duration increased to 23 ns. The distortion of initial acoustic pulse was significant. The change in ultrasonic pulse shape indicates an influence of the acoustic attenuation on pressure profiles.

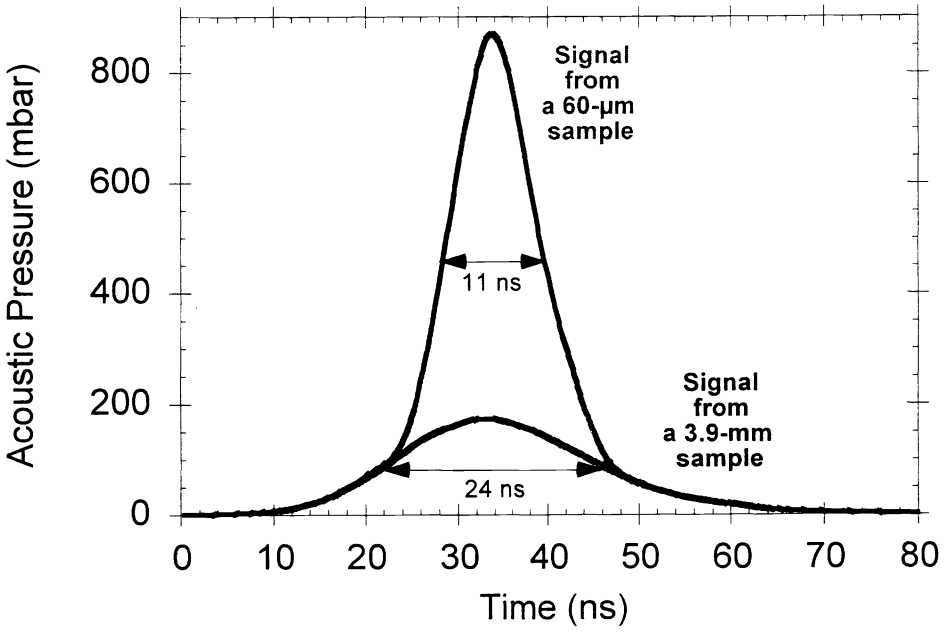

Figure 6. Optoacoustic pressure profile measured from bovine liver with different thickness.

Figure 7 shows pressure amplitude as a function of liver thickness. A strong acoustic attenuation was observed, when acoustic pulses propagated first several hundred microns in the liver samples. A lower attenuation was observed if the pulses propagate longer distance. The experimental data were fit with a function representing a sum of two exponents. The fit determined the attenuation coefficient of 7.1 mm^{-1} within the fraction of millimeter and 0.26 mm^{-1} for the distances of several millimeters.

5. DISCUSSION

5.1. Breast phantom experiment.

The accuracy of localization and diameter measurement was in the range of a fraction of millimeter for the spherical acoustic sources in the breast phantoms. Therefore, z-axial resolution was equal to a fraction of millimeter in this case. It is limited by the temporal response of the acoustic transducer. This resolution is enough for accurate localization of spherical sources and measurements of their dimensions at the distance of several centimeters . This statement is valid, if the distance between the spherical sources and the transducer is greater than the characteristic dimensions of the transducer. If the distance is comparable to the transducer dimensions, the resolution is lower due to pressure pulse distortion.

5.2. Acoustic diffraction experiment.

The experiment on diffraction demonstrated that z-axial resolution can be up to 20 μm even for strongly diffracted signals. It is very close to the z-axial resolution for ideal plane wave limited by the temporal response of acoustic transducers

and the electronic detection system, and the laser pulse duration. We demonstrated that measurements of dimensions and location of tissue layers are insignificantly influenced by diffraction effects. Application of diffraction correction algorithms are not necessary in case when only z-axial resolution is concerned.

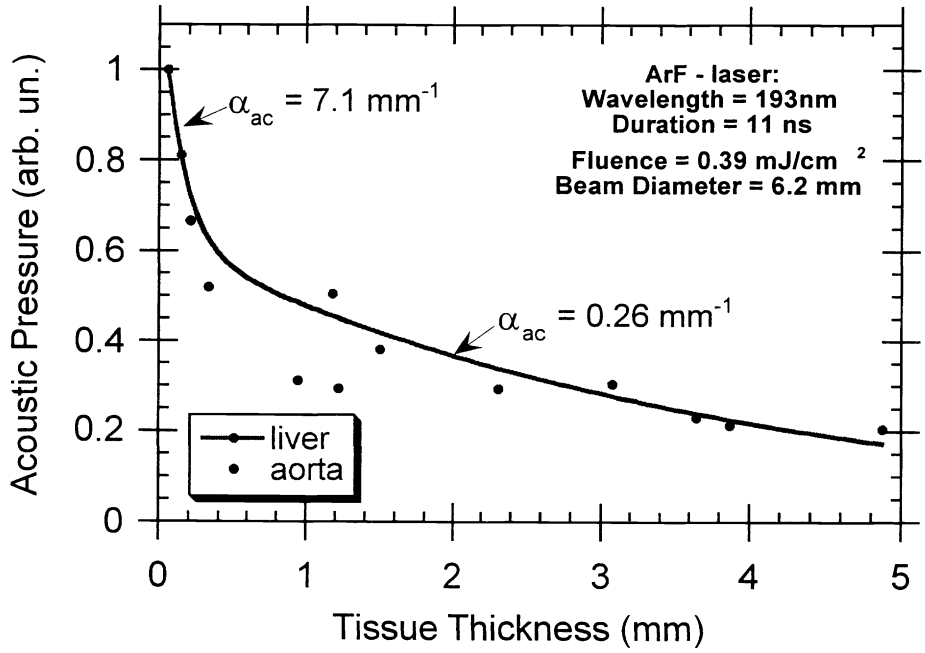

Figure 7. A ultrasonic pulse pressure amplitude as a function of thickness for a liver slab and an aorta wall. Two major ultrasonic frequency components may be delineated in the curve (exp fit is shown for the liver slab only).

5.3. Acoustic attenuation experiment.

The data on acoustic attenuation demonstrated strong attenuation of high-frequency component in the pressure pulses at distances of the order of 100 μm. A low-frequency component was attenuated at the distances of the order of several millimeters. These data are consistent with the fact that the acoustic attenuation coefficient for high-frequency waves is greater than that for low-frequency ultrasonic waves.

The position of the irradiated tissue surface can be calculated using the formula (4) from the position of the maximum in the pressure profiles. The axial resolution for thin samples was about 15 μm as defined by a longest of threee times: the temporal resolution of the transducer, the response of detection system, and the laser pulse duration. The ultrasonic pulse propagated through a 3.9-mm liver sample was 13-ns wider that the initially generated pulse. Therefore, resolution was 20 μm in this case.

The generated pressure profiles can be reconstructed from the detected one if acoustic attenuation is known at different frequencies. This can decrease acoustic attenuation effects and improve z-axial resolution of laser optoacoustic imaging.

6. CONCLUSION

This study demonstrated that acoustic diffraction decreases insignificantly the z-axial resolution of the laser optoacoustic imaging. The accuracy of dimensions measurement in laser optoacoustic imaging is defined by the widening of ultrasonic pulses upon propagation in tissues due to a stronger attenuation of high ultrasonic frequencies. The thickness of an absorbing layer within our phantom was measured with a 20-μm precision. The axial resolution was approximately 0.5 mm in breast phantoms with characteristic dimension of 10 cm.

Acoustic transducer aperture may also decrease the resolution, if it is comparable to the distance between the spherical source and the transducer. In the case of spherical sources located far from the transducer, the resolution is not influenced by its aperture and defined by its temporal response and bandwidth of detection system.

7. ACKNOWLEDGMENTS

This work is supported in part by grants from the Whitaker Foundation and the Advanced Technology Program of the Texas Higher Education Coordinating Board.

8. REFERENCES

1. "Optical Tomography, Photon Migration, and Spectroscopy of Tissue and Model Media: Theory, Human Studies, and Instrumentation," *Proc. SPIE* **2389**, 1995; "Optical Tomography and Spectroscopy of Tissue: Theory, Instrumentation, Model and Human Studies," *Proc. SPIE* **2979**, 1997.
2. *"OSA Proceedings on Advances in Optical Imaging and Photon Migration,"* (R. R. Alfano, ed.), **21**, 1994; *"OSA Trends in Optics and Photonics on Advances in Optical Imaging and Photon Migration,"* R. R. Alfano and J. G. Fujimoto, eds. (OSA, Washington, DC), **2**, 1996.
3. R.C. Sanders: "Clinical (ultra)sonography: a practical guide", Little & Brown, Boston, 1991
4. F. A. Duck, "*Physical properties of tissue: A comprehensive reference book*", Academic Press, San Diego, 1990.
5. A.A. Oraevsky, R.O. Esenaliev, S.L. Jacques, F.K. Tittel: Laser Opto-Acoustic Tomography for medical diagnostics: principles, *Proc. SPIE* 1996; **2676**: 22-31.
6. A.A. Oraevsky, S.L. Jacques, F.K. Tittel: Determination of tissue optical properties by time-resolved detection of laser-induced stress waves. *Proc. SPIE* 1993; **1882**: 86-101.
7. A.A. Oraevsky, S.L. Jacques, F.K. Tittel: Measurement of tissue optical properties by time-resolved detection of laser-induced transient stress, *Applied Optics,* 1997; **36**(1): 402-415.
8. A.A. Oraevsky: Laser optoacoustic imaging for cancer diagnosis, *LEOS NewsLetter* 1996; **12**: 17-20.
9. R.O. Esenaliev, A.A. Oraevsky, S.L. Jacques, F.K. Tittel: Laser Opto-Acoustic Tomography for medical diagnostics: experiments with biological tissues, *Proc. SPIE* 1996; **2676**: 84-90.
10. R.O. Esenaliev, F.K. Tittel, S.L. Thomsen, B. Fornage, C. Stelling, A.A. Karabutov, and A.A. Oraevsky: Laser optoacoustic imaging for breast cancer diagnostics: Limit of detection and comparison with X-ray and ultrasound imaging, *Proc. SPIE* 1997; **2979**: 71-82.
11. A. A. Oraevsky, R. O. Esenaliev, S. L. Jacques, and F. K. Tittel: "Lateral and z-axial resolution in laser optoacoustic imaging with ultrasonic transducers", *Proc. SPIE*, **2389**, pp. 198-208, 1995.
12. C.G.A. Hoelen, R.Pongers, G. Hamhuis, F.F.M. deMul, J. Greve: Photoacoustic blood cell detection and imaging of blood vessels in phantom tissue, Proc. SPIE 3196: 142-153, 1997.
13. G. J. Diebold and T. Sun. "Properties of optoacoustic waves in one, two, and three dimensions", *Acustica*, **80**, pp. 339-351, 1994.
14. A. A. Oraevsky, R. O. Esenaliev, S. L. Jacques, F. K. Tittel, and D. Medina: "Breast Cancer Diagnostics by Laser Opto-Acoustic Tomography", *OSA Trends in Optics and Photonics on Advances in Optical Imaging and Photon Migration,"* R. R. Alfano and J. G. Fujimoto, eds. (OSA, Washington, DC), **2**, pp. 316-321, 1996.
15. V. E. Gusev and A. A. Karabutov. "Laser Optoacoustics", AIP Press, New York, 1993.
16. A.A. Karabutov, N.B. Podymova, V.S. Letokhov: "Time-resolved laser optoacoustic tomography of inhomogeneous media", *Applied Phys. B* vol. **63**: 545-563, 1996.
17. S. A. Goss, R. L. Johnston, and F. Dunn. "Comprehensive compilation of empirical ultrasonic properties of mammalian tissues", *J. Acoust. Soc. Am.*, **64(2)**, pp. 423-457, 1978.
18. M.W. Sigrist: Laser generation of acoustic waves in liquids and gases, J. Appl. Phys. 60: R83-R121, 1986.
19. G. Paltauf, H. Schmidt-Kloiber, H. Guss: Light distribution measurement in absorbing materials by optical detection of laser-induced stress waves, Appl. Phys. Lett. 69: 1526-1528, 1996.
20. J. Kolzer, G. Mitic, J. Otto, and W. Zinth. "Measurements of the optical properties of breast tissue using time resolved transillumination", *Proc. SPIE*; **2326**, pp. 143-152, 1994.
21. K. Suzuki, Y. Yamashita, K. Ohta, M. Kaneko, M. Yoshida, and B. Chance. "Quantitative measurement of optical parameters in normal breasts using time-resolved spectroscopy: *in vivo* results of 30 Japanese women", *J. Biomed. Optics,* **1(3)**, pp. 330-334, 1996.